Superconducting and structural properties of the type-I superconductor PdTe2 under high pressure

Furue, Y.; Fujino, T.; Salis, M.V.; Leng, H.; Ishikawa, F.; Naka, T.; Nakano, S.; Huang, Y.; de Visser, A.; Ohmura, A.

DOI
10.1103/PhysRevB.104.144510

Publication date
2021

Document Version
Final published version

Published in
Physical Review B

Superconducting and structural properties of the type-I superconductor $PdTe_2$ under high pressure

Yusaku Furue,[1] Tadachika Fujino,[2] Marc V. Salis,[3] Huaqian Leng,[3,4] Fumihiro Ishikawa,[2] Takashi Naka,[5] Satoshi Nakano,[5] Yingkai Huang,[3] Anne de Visser,[3] and Ayako Ohmura[2,*]

[1]*Graduate School of Science and Technology, Niigata University, 8050, Ikarashi 2-no-cho, Nishi-ku, Niigata 950-2181, Japan*
[2]*Faculty of Science, Niigata University, 8050, Ikarashi 2-no-cho, Nishi-ku, Niigata 950-2181, Japan*
[3]*Van der Waals-Zeeman Institute, University of Amsterdam, Science Park 904, 1098 XH Amsterdam, The Netherlands*
[4]*School of Physics, University of Electronic Science and Technology of China, Chengdu 610054, China*
[5]*National Institute for Materials Science (NIMS), Sengen 1-2-1, Tsukuba, Ibaraki 305-0047, Japan*

(Received 11 August 2021; accepted 4 October 2021; published 25 October 2021)

The transition metal dichalcogenide $PdTe_2$ has attractive features based on its classification as a type-II Dirac semimetal and the occurrence of type-I superconductivity, providing a platform for discussion of a topological superconductor. Our recent work revealed that type-I superconductivity persists up to pressures of ∼2.5 GPa and the superconducting transition temperature T_c reaches a maximum at around 1 GPa, which is inconsistent with the theoretical prediction. To understand its nonmonotonic variation and investigate superconductivity at higher pressures, we performed structural analysis by x-ray diffraction at room temperature below 8 GPa and electrical resistivity measurements at low temperatures from 1 to 8 GPa. With regard to the superconductivity beyond 1 GPa, the monotonic decrease in T_c is reproduced without any noticeable anomalies; T_c changes from 1.8 K at 1 GPa to 0.82 K at 5.5 GPa with $dT_c/dP \sim -0.22$ K/GPa. The crystal structure with space group $P\bar{3}m1$ is stable in the pressure range we examined. On the other hand, the normalized pressure-strain analysis (finite strain analysis) indicates that the compressibility changes around 1 GPa, suggesting that a Lifshitz transition occurs. We here discuss the effect of pressure on the superconducting and structural properties based on the comparison of these experimental results.

DOI: 10.1103/PhysRevB.104.144510

I. INTRODUCTION

The family of transition metal dichalcogenides attracts much attention because of their versatile electronic properties. Notably, some members are classified as a type-II Dirac semimetal, which implies a tilted Dirac cone, resulting in the breaking of Lorentz invariance, with a topologically nontrivial surface state [1–3]. Of particular interest in the family is $PdTe_2$, which is well known as a superconductor at ambient pressure [4]. The coexistence of characteristic electronic states with a nontrivial nature, which was experimentally confirmed [3,5–9], in combination with superconductivity, enhances its reputation as a potential topological superconductor, and as such provides a platform for discussion of the relationship between superconducting properties and Dirac fermions.

The superconducting properties of $PdTe_2$ have been widely investigated at ambient pressure [7,8,10–19]. $PdTe_2$ is a type-I superconductor with $T_c = 1.64$ K, and its critical field $\mu_0 H_c(T)$ follows the standard quadratic temperature variation with $\mu_0 H_c(0) = 13.6$ mT [10]. The bulk superconducting property is found to be of conventional nature with a full superconducting gap confirmed by heat capacity [11,19] and penetration depth measurements [12,13]. Furthermore, it is considered that a saddle-point van Hove singularity (vHs) near the M point in the Brillouin zone, which is located about 30 meV above the Fermi level [20], plays an important role in the conventional Bardeen-Cooper-Schrieffer (BCS) behavior [14]. Meanwhile, as regards the surface states of $PdTe_2$, its superconducting properties are under discussion [7,8,10,15–17]. Leng *et al.* observed an unusual surface sheath superconductivity in ac-susceptibility measurements in magnetic fields [10]. Its critical temperature is estimated to be $T_c^S \sim 1.3$ K and persists up to $\mu_0 H_c^S(0) = 34.9$ mT, which is higher than the bulk critical field $\mu_0 H_c(0)$. This anomalous behavior cannot be explained by the standard Saint-James–de Gennes model for surface superconductivity [21]. Specifically, in the standard theory, provided that the Ginzburg-Landau parameter κ (equal to the penetration depth λ divided by the coherence length ξ) is smaller than 0.42 in a type-I superconductor, the critical field of surface superconductivity should be smaller than that of the bulk. In the case of $PdTe_2$, despite the fact that $\kappa \sim 0.09$–$0.28 < 0.42$ [10,12], $\mu_0 H_c^S(0)$ is larger than $\mu_0 H_c(0)$. This suggests that the surface sheath could have an unusual topological nature. In contrast, spectroscopic measurements such as scanning tunneling microscopy and scanning tunneling spectroscopy (STM-STS) and point-contact spectroscopy, which are genuine surface probes, reported that the surface superconductivity is conventional and no in-gap states exist [7,8,15–17]; different views on the superconductivity are, however, that it exhibits type-II behavior [7] or a mixture of type-I and type-II behavior [15,17].

*ohmura@phys.sc.niigata-u.ac.jp

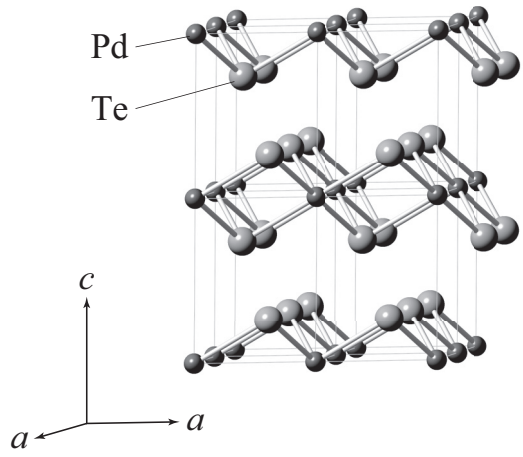

FIG. 1. The crystal structure of $PdTe_2$ at ambient conditions with space group $P\bar{3}m1$ (No. 164). Green and gray spheres indicate the Pd and Te atoms, respectively.

Since applying pressure can continuously tune structural and electronic states of materials, it is a most useful probe in research on superconductors and topological quantum materials. The effects of pressure on $PdTe_2$ have already been reported in several papers [22–25]. $PdTe_2$ crystallizes in a layered structure with space group $P\bar{3}m1$ ($a = 4.037(2)$ Å, $c = 5.132(2)$ Å [22] at ambient conditions) as shown in Fig. 1. The Te-Pd-Te layers are weakly bonded by van der Waals interaction. Soulard *et al.* reported that the $P\bar{3}m1$ structure is maintained up to pressures of 27 GPa at room temperature [22]. First-principles calculations using the structural parameters of Ref. [22] predicted a monotonic depression of superconductivity up to pressures of 10 GPa, which is attributed to the decrease in density of states and the blueshift of the phonon frequency induced by pressure [23]. In our previous work, we found that the pressure variation of the transition temperature $T_c(P)$ differs from that of the theoretical prediction; T_c reaches a maximum value of 1.91 K at 0.91 GPa and then decreases to 1.27 K at 2.49 GPa [24]. To understand this result, we investigated the carrier density n under pressure first. However, the variation of n does not explain $T_c(P)$ because n shows only a slight increase as a function of pressure (see the Supplementary Material in Ref. [24]). On the other hand, an enhancement of T_c is also reported in studies on Cu-intercalated Cu_xPdTe_2 ($T_c^{max} = 2.6$ K for $x = 0.06$) [26] and the Au-substituted series $Au_{1-x}Pd_xTe_2$ ($T_c^{max} = 4.65$ K for $x = 0.40$) [27]. We traced the relative change in T_c as a function of the relative volume change in Fig. 7 of Ref. [24]. Though the value of T_c basically decreases with a smaller volume, the positive pressure variation of T_c up to 0.91 GPa is at odds with this trend, and its origin remains unresolved.

Additionally, a pressure-induced topological transition is theoretically predicted at higher pressures by Xiao *et al.*; a type-I Dirac point appears at 4.7 GPa near the Γ point, and the type-II Dirac point near the A point disappears at 6.1 GPa due to the pressure-induced shifts of the electronic bands [23]. Very recently, Yang *et al.* reported that there is no anomalous behavior in the temperature dependence of the resistivity up to pressures of 8.2 GPa [25]. However, the pressure variation of T_c is yet to be revealed in this pressure range since the data in their research were taken at $T > 2$ K.

In this paper, we focus on elucidating the origin of the nonmonotonic variation of T_c and investigate superconductivity at higher pressures where the occurrence of a topological transition is expected. Furthermore, the detailed structural information below 2.5 GPa is also necessary to reveal the origin of the nonmonotonic $T_c(P)$, because the structural parameters of $PdTe_2$ below 2.5 GPa were not taken in Ref. [22]. For this purpose, the effects of pressure on the structural and superconducting properties of $PdTe_2$ up to pressures of 8 GPa were examined by synchrotron radiation x-ray diffraction and electrical resistivity measurements, respectively.

II. EXPERIMENTS

The $PdTe_2$ crystals used in the present study were taken from a single-crystalline boule prepared under the modified Bridgman technique [28]. Scanning electron microscopy with energy dispersive x-ray (EDX) spectroscopy shows the proper 1:2 stoichiometry within the experimental resolution of 0.5% (see the Supplemental Material in Ref. [10]). The superconducting properties at ambient pressure were characterized in Ref. [10].

A diamond anvil cell (DAC) was used for x-ray diffraction (XRD) under high pressure. A culet anvil of 0.75 mm diameter was selected to fine-tune the experimental pressure in the range below 8 GPa. A powder sample of $PdTe_2$ was prepared by grinding fragments cut out of a single crystal. It was placed in a sample space, 255 μm in diameter and 96 μm thick, made by drilling a small hole in a SUS301 gasket. We performed the XRD study twice utilizing different pressure-transmitting mediums. For hydrostatic compression, a 4:1 mixture of methanol (MeOH) and ethanol (EtOH) was loaded into the sample room together with the power sample in the first run, whereas fluid helium (He) compressed to ∼180 MPa was used in the second run [29]. XRD with synchrotron radiation was carried out at beamline AR-NE1A of Photon Factory of the High-Energy Accelerator Research Organization (KEK) in Tsukuba, Japan. An incident beam was tuned to an energy of ∼29.7 keV ($\lambda \sim 0.417$ Å) and beam size of 75×75 μm^2. An imaging plate was used as a detector (Rigaku R-AXIS IV). All of the diffraction patterns under high pressures were measured at room temperature. Values of the applied pressures were determined using the ruby fluorescence method. The Rietveld analysis to obtain structural parameters was performed with the crystallographic program JANA2006 [30,31]. A typical analytical result that gives a good fit is shown in Fig. S1 of the Supplemental Material (SM) [32].

Electrical resistivity measurements under high pressures and low temperatures were performed utilizing a Cu-Be modified Bridgman anvil cell [33–35]. The $PdTe_2$ sample was put into a Teflon capsule together with a mixture of Fluorinert (FC70:FC77 = 1:1), which is a pressure-transmitting medium used for quasihydrostatic compression. The pressure value generated in the capsule against the load on the high-pressure cell was calibrated in advance by the critical pressures of the structural phase transitions in elemental bismuth (purity 5N). The $PdTe_2$ samples were cut out of a bigger single crystal; the typical size is $\sim 0.3 \times 0.7 \times 0.1$ mm^3 (width × length ×

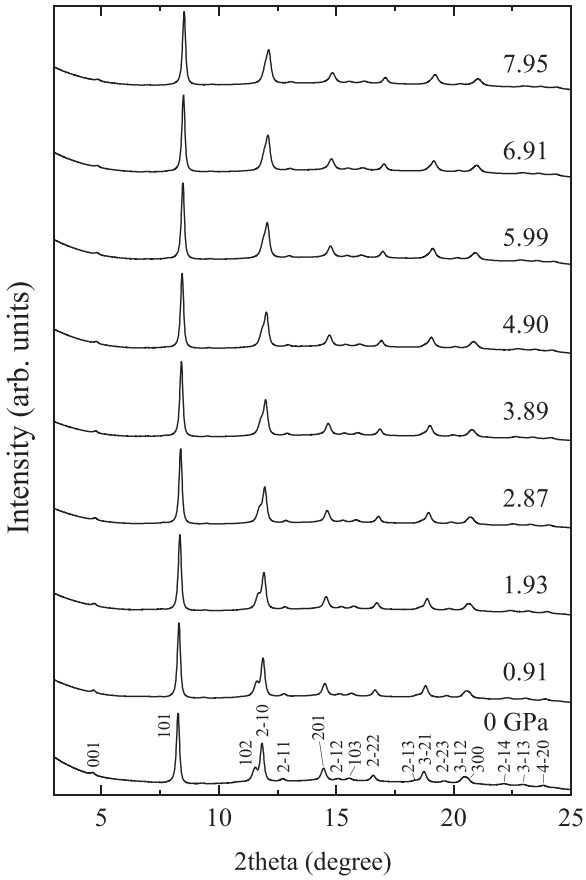

FIG. 2. Diffraction patterns of $PdTe_2$ measured in the first run with increasing pressure at room temperature.

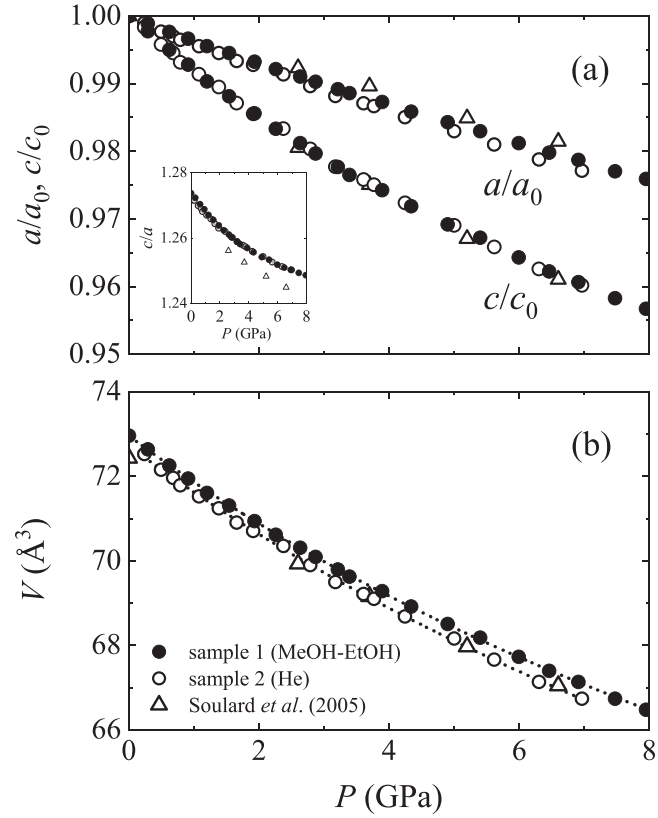

FIG. 3. Pressure variation of the normalized lattice constants (a) and the unit-cell volume (b). The inset in (a) shows the ratio c/a as a function of pressure. Values shown as closed and open circles were obtained in the first and second run, respectively. Open triangles show the experimental values reported by Soulard *et al.* [22]. Dotted lines in (b) are the results of a fit to the BM-EOS (see text).

height). We measured the temperature variation of the resistivity, $\rho(T)$, of three samples under high pressure. These samples were compressed at room temperature, and then the $\rho(T)$ curves at each pressure were measured under the following temperature conditions: sample 1 (the first run) at temperatures of $T \geqslant 1.9$ K [in a physical property measurement system (PPMS), Quantum Design], sample 2 (the second run) at $T \geqslant 0.8$ K (using a ^{3}He-circulation–Joule-Thomson type Gifford-McMahon cryogenic refrigerator, Iwatani Industrial Gases), and sample 3 (the third run) at $T \geqslant 0.3$ K (in a ^{3}He refrigerator, Oxford Instruments Heliox VL).

III. RESULTS

A. X-ray diffraction

Figure 2 shows the pressure variation of the XRD patterns of $PdTe_2$ with increasing pressure taken in the first run. All reflections are indexed with $P\bar{3}m1$ symmetry. The diffraction pattern shifts to a higher scattering angle due to shrinkage of the crystal lattice, and its profile is basically kept up to the highest pressure, indicating that no structural phase transition occurs in this range as reported in Ref. [22]. The 102 reflection merges into the $2\bar{1}0$ one, suggesting that the c axis of the $P\bar{3}m1$ structure is more compressible than the a axis.

Figure 3(a) shows the normalized lattice constants a/a_0 and c/c_0 as a function of pressure: $a_0 = 4.0441(1)$ Å and $c_0 = 5.1511(4)$ Å at 0 GPa measured in the first run. The experimental data obtained in this paper are plotted together with those of Ref. [22], and their variations are consistent with each other. Both a and c monotonically decrease with pressure. The ratio of lattice constants c/a shown in the inset of Fig. 3(a) also varies without an extremum. This suggests that the larger shrinkage of the crystalline lattice along the c axis continues up to pressures of 8 GPa in $PdTe_2$. The compression curve can be fitted by the Birch-Murnaghan equation of state (BM-EOS) as shown in Fig. 3(b) [36]:

$$P = \frac{3}{2}B_0\left\{\left(\frac{V_0}{V}\right)^{\frac{7}{3}} - \left(\frac{V_0}{V}\right)^{\frac{5}{3}}\right\} \times \left[1 + \frac{3}{4}(B_0' - 4)\left\{\left(\frac{V_0}{V}\right)^{\frac{2}{3}} - 1\right\}\right],$$

where V_0 and V are volumes at ambient and high pressures, P is in units of gigapascals, B_0 is the bulk modulus, and B_0' is its pressure derivative. The fits for the first and second runs give parameters $B_0 = 62.9(9)$ and 59(2) GPa and $B_0' = 6.7(2)$ and 7.0(2), respectively, for $PdTe_2$ with the $P\bar{3}m1$ structure. The pressure error in the second run is a little larger than that of the first run, which is reflected in the error of B_0. Compared with Ref. [22], the value of the bulk modulus in this paper is smaller than theirs, $B_0 = 101.5$ GPa. This is attributed to the

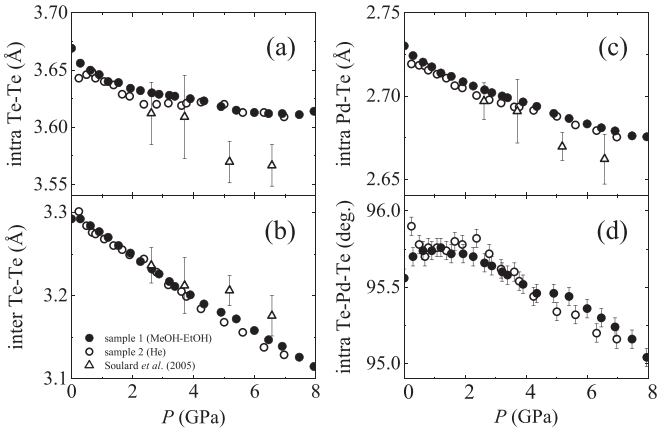

FIG. 4. Pressure dependences of the atomic spacings and bond angle in $PdTe_2$: (a) intralayer (intra) Te-Te, (b) interlayer (inter) Te-Te, (c) intralayer Pd-Te spacings, and (d) intralayer Te-Pd-Te angle. Closed and open circles indicate values obtained in the first and second run, respectively. Open triangles show experimental values reported by Soulard *et al.* [22].

difference in whether or not the volume at ambient pressure is fixed as a fitting parameter and the pressure range used for the fitting of the equation of state.

Figure 4 shows the atomic spacings and bond angle of $PdTe_2$ with increasing pressure: intralayer Te-Te [Fig. 4(a)], interlayer Te-Te [Fig. 4(b)], intralayer Pd-Te spacings [Fig. 4(c)], and intralayer Te-Pd-Te angle [Fig. 4(d)]. In $PdTe_2$, the atomic positions in the unit cell are $1a$ $(0, 0, 0)$ for Pd and $2c$ $(1/3, 2/3, z_{\mathrm{Te}})$ for Te, respectively; only z_{Te} can be optimized, and its value at 0 GPa is $z_{\mathrm{Te}} = 0.2747(5)$. The interlayer Te-Te and intralayer Pd-Te spacings shown in Figs. 4(b) and 4(c) indicate a monotonic decrease with pressure. Since the interlayer spacings in $PdTe_2$ are due to weak bonds by the van der Waals force, the interlayer Te-Te spacing is about three times more compressible than other intralayer spacings. Meanwhile, the pressure variations of the intralayer Te-Te spacing and intralayer Te-Pd-Te angle show small nonmonotonic changes. In particular, the angle hardly changes below $\sim$2 GPa and decreases beyond this pressure, though the values around 0.3 GPa in the first and second runs deviate slightly from the overall trend. From Table S1 of the SM [32], it can be concluded that the value of z_{Te} approximately remains constant within the error up to $\sim$1.2 GPa and subsequently starts to increase with pressure. The intralayer Te-Pd-Te angle tends to increase up to $\sim$1.2 GPa, since the unit cell is more compressible along the c axis. The extracted pressure variations of the atomic spacings are in agreement with literature data basically [22]. The difference in values above 4 GPa is probably caused by the degree of hydrostaticity, which is due to the solidification of the nitrogen used as a pressure-transmitting medium in Ref. [22].

B. Electrical resistivity

We measured the pressure variation of the electrical resistivity on three samples. In the first run, shown in Fig. 5(a), a drop in the resistance corresponding to a superconducting transition was observed above 3.7 GPa, though zero resistance was not attained. At this pressure, the transition is fairly broad and has three steps at 3.5, 3.0, and 2.6 K, suggesting an inhomogeneous superconducting state. On further compression, the superconducting transition shifts to higher temperatures at 4.5 GPa and is subsequently depressed and changes to a single-step transition up to pressures of 7.5 GPa. As mentioned in the Introduction, the appearance of the type-I Dirac point is theoretically predicted at 4.7 GPa. We therefore performed two more pressure runs to investigate the reproducibility of this higher-T_c phase. Figure 5(b) shows the pressure variation of the electrical resistivity obtained in the second run. A sharp transition is observed at $T_c = 1.8$ K at 1 GPa, which is the lowest experimental pressure in this run. The superconductivity is depressed with pressure, and T_c decreases to 0.82 K at 5.5 GPa. Above T_c the normal state resistance is close to temperature independent, and the anomalous behavior in the first run is not reproduced.

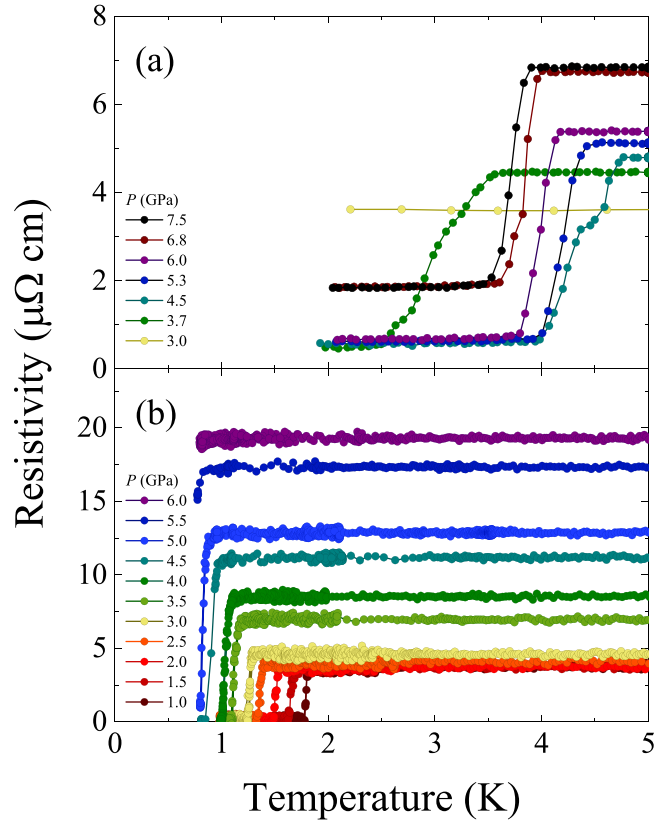

FIG. 5. Temperature dependence of the electrical resistivity of $PdTe_2$ obtained in the first run (a) and second run (b) with increasing pressure up to 7.5 and 6.0 GPa, respectively. The measurement temperature ranges are (a) $T \geqslant 2$ K and (b) $T \geqslant 0.8$ K, respectively.

The pressure variation in the third run reproduces the one in the second run. Figure 6 shows the onset temperatures of the superconducting transitions obtained in the three runs (and samples), T_c^{R1}, T_c^{R2}, and T_c^{R3}, plotted together with T_c^R and T_c^χ from our previous work [24]. T_c^{R2} monotonically decreases with pressure derivative $dT_c^{R2}/dP \sim -0.22$ K/GPa. T_c^{R3} also follows this variation under pressure, though between 2 and 3 GPa the data points lie a little lower. Furthermore, these values and pressure variations are consistent with those of T_c^R and T_c^χ. Therefore it can be concluded that T_c^{R2} and T_c^{R3} must

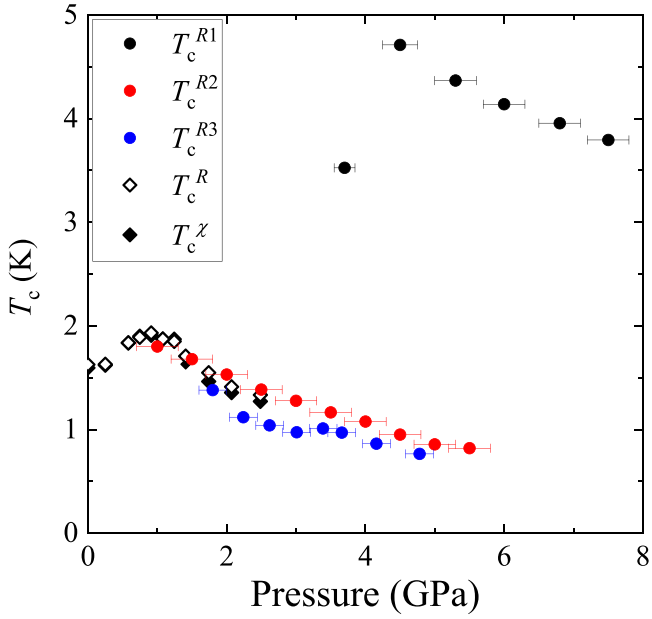

FIG. 6. Pressure variation of the superconducting transition temperature of $PdTe_2$. Black, red, and blue closed circles indicate the onset temperatures obtained in the first (T_c^{R1}), second (T_c^{R2}), and third (T_c^{R3}) run, respectively. Open and closed diamonds indicate T_c obtained in our previous resistivity (T_c^{R}) and ac-susceptibility (T_c^{χ}) measurements [24].

be attributed to the bulk superconducting phase of $PdTe_2$ and that the depression of this superconducting phase above 1 GPa is an intrinsic property. On the other hand, the superconducting phase with T_c^{R1} was observed only in the first run. Since the pressure variation of T_c^{R1} is clearly distinct, we infer that the superconductivity related to T_c^{R1} does not originate from $PdTe_2$, as will be discussed later.

Figure 7 shows the electrical resistivity versus temperature normalized to its value at room temperature, $\rho(T)/\rho(\mathrm{RT})$,

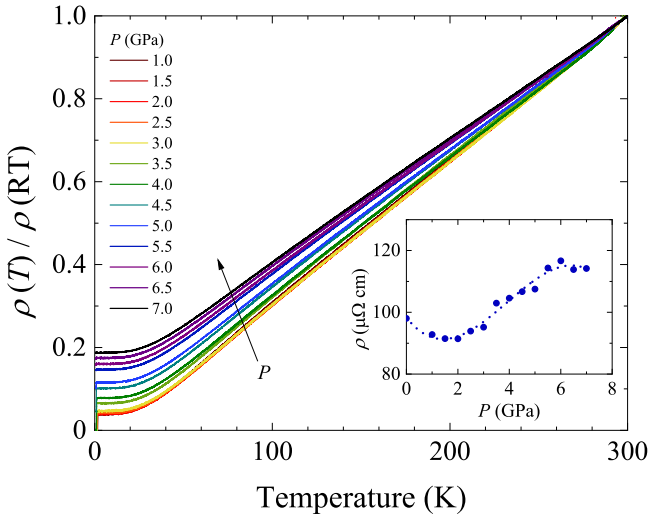

FIG. 7. Pressure dependence of the electrical resistivity normalized to its value at room temperature $\rho(\mathrm{RT})$ taken in the first run. The inset shows $\rho(\mathrm{RT})$ as a function of pressure.

obtained in the second run. The temperature dependence of the resistivity shows metallic behavior, and no anomalies are observed up to 7.0 GPa. This behavior in $\rho(T)/\rho(\mathrm{RT})$ is consistent with the behavior reported by Yang *et al.* [25]. The resistivity at room temperature is 98 $\mu\Omega$ cm at ambient pressure and shows a minimum value around 2 GPa on compression as shown in the inset of Fig. 7. Furthermore, we estimated the Debye temperature Θ_D utilizing two sets of $\rho(T)$ data, which were obtained on sample 2 and another sample [sample 4, $0.4 \leqslant P$ (GPa) $\leqslant 2.4$]. Each $\rho(T)$ curve can be fitted to the Bloch-Grüneisen formula based on electron-phonon scattering. Θ_D keeps values of ~184.8(6) K up to 1 GPa and then gradually increases with ~15 K/GPa up to ~3 GPa. A typical fitting result at 0.4 GPa on sample 4 and the pressure variation of Θ_D are shown in Figs. S2 and S3 of the SM [32], respectively.

IV. DISCUSSION

First, we discuss the superconducting phase with T_c^{R1} that appeared above a pressure of 3.7 GPa in the first run. It is tempting to relate this higher-T_c phase to the occurrence of the pressure-induced topological transition from a type-II to a type-I Dirac semimetal that was predicted by Xiao *et al.* [23]. At such a transition, the tilt parameter k of the Dirac cone reaches a critical value of 1, and superconductivity is enhanced [37]. However, as mentioned before, this higher-T_c phase has not been reproduced in the two subsequent runs. Furthermore, the pressure variation of the electrical resistivity at room temperature is also different for samples 1 and 2 as shown in Fig. S4 of the SM [32]; the resistivity of sample 1 monotonically decreases with pressure, while that of sample 2 increases above 2 GPa as shown in the inset of Fig. 7. These results suggest that the higher-T_c superconductivity is not caused by $PdTe_2$, but by another component. It is therefore concluded that the monotonic depression of the original superconductivity shown as T_c^{R2} and T_c^{R3} is the intrinsic behavior from 1 to 6 GPa in $PdTe_2$, and no indications related to the topological transition are observed in the resistivity measurements.

Here, we argue that T_c^{R1} can likely be attributed to the pressure-induced superconductivity of tellurium (Te). According to a past report [38], superconductivity in pure Te emerges above $P \sim 4$ GPa, and its pressure variation is very similar to that of T_c^{R1}; T_c of pure Te increases from 3.4 K at ~4 GPa to 4.3 K at ~6 GPa and then gradually decreases to 2.8 K at ~15 GPa [38]. Possibly, some trace amounts of elemental Te cause filamentary superconductivity under pressure. We remark that the Te content was below the threshold for detection by EDX spectroscopy. The multistep superconducting transition is compatible with this idea. The x-ray diffraction results under pressure indicate that the amount of the Te impurity phase must be very small, since no reflections related to Te have been observed.

Next, the nonmonotonic variation of the superconducting transition temperature below 2 K, where T_c passes through the maximum of 1.91 K at 0.91 GPa, is discussed. In general, applying pressure tends to depress superconductivity. On the other hand, an increase in T_c under pressure has been observed in several transition metal chalcogenides, e.g., MX_2 (M =

Ni, Pd, Nb; X = S, Se, Te) and $ZrTe_3$ [39–43]. The effect of pressure on superconductivity has often been discussed based on the following points [44,45]: (1) The sign of dT_c/dP depends on the magnitude of the Hopfield parameter η for electronic properties and the Grüneisen parameter γ for lattice hardening, and (2) a variation of the energy bands near the Fermi energy E_F can contribute to a change in the density of states and also cause a pressure-induced electronic transition, which can alter the superconducting properties.

We here consider the first point qualitatively. The sign of dT_c/dP is expected to become positive when the logarithmic volume derivative of $\eta = N(E_f)\langle I^2\rangle$ is larger in magnitude than two times $\gamma = -d\ln\langle\omega\rangle/d\ln V$ [45], where $N(E_f)$ is the electronic density of states at the Fermi level, $\langle I^2\rangle$ is the average square electronic matrix element, and $\langle\omega\rangle$ is the average phonon frequency. The carrier density in $PdTe_2$ at 2 K undergoes a quasilinear increase by ~20% up to a pressure of ~2.1 GPa without any anomalous behavior around 0.9 GPa, where $T_c(P)$ has a maximum (see the Supplementary Material in Ref. [24]). Meanwhile, as mentioned before, Θ_D, proportional to $\langle\omega\rangle$, changes little up to ~1 GPa, which results in a very small value of γ. From these two points, the required condition for $dT_c/dP > 0$ might be fulfilled below 1 GPa. Beyond this pressure, the rise in Θ_D makes γ larger, overwhelming the moderate increase in $N(E_f)$, and thereby results in the depression of superconductivity. Based on this idea, the value of $d\ln\eta/d\ln V$ below 2.5 GPa can be estimated to be approximately −2.9 for $\gamma \sim 0$ at $P < 1$ GPa and approximately −2.8 for $\gamma \sim 3.3$ at $P > 1$ GPa, respectively (see Sec. 4 of the SM [32]). The variation of $d\ln\eta/d\ln V$ is very small and consistent with those of carrier density.

Next, we will examine the second point for the enhancement of superconductivity. Since $PdTe_2$ shows no structural phase transition up to pressures of 8 GPa, we explore the possibilities of an electronic transition. For this purpose, a normalized pressure H_v versus a Eulerian strain f_E was calculated by employing the experimental lattice constants in the following formula:

$$H_v = \frac{P}{3f_E(1+2f_E)^{\frac{5}{2}}}, \quad f_E = \frac{1}{2}\left[\left(\frac{V_0}{V}\right)^{\frac{2}{3}} - 1\right],$$

where V_0 and V are volumes at ambient and high pressure, respectively, P is in units of gigapascals, and

$$H_v = B_0 + \tfrac{3}{2}B_0(B_0' - 4)f_E,$$

where B_0 is the bulk modulus and B_0' is its pressure derivative. As noted above, H_v and f_E have a linear relationship via B_0 and B_0'. The intercept of the linear fit to $H_v(f_E)$ and the axis at $f_E = 0$ gives an estimate of the bulk modulus in each region. Additionally, a change in the slope of $H_v(f_E)$ indicates a modification of the topology of the Fermi surface, suggesting that a Lifshitz transition occurs [46–48].

Figure 8 shows $H_v(f_E)$ obtained in two runs utilizing different pressure-transmitting mediums. The variation of $H_v(f_E)$ can be approximated by three straight lines with a different slope. This behavior is particularly noticeable in sample 2. A change in the slope occurs at $f_E \sim 0.006$ ($P \sim$ 1.2 GPa) and 0.008 (1.6 GPa) for sample 1 and at $f_E \sim 0.004$ ($P \sim 0.9$ GPa) and 0.007 (1.3 GPa) for sample 2. Especially,

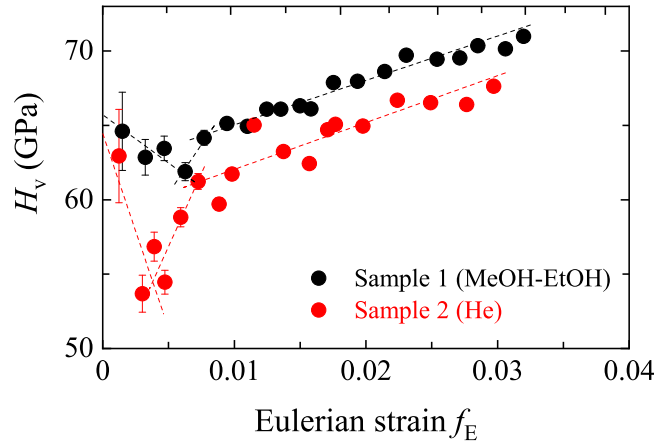

FIG. 8. Plot of the normalized pressure H_v vs the Eulerian strain f_E at ambient temperature. Black and red colors indicate data calculated from the first (sample 1) and second (sample 2) runs measured utilizing the mixture of MeOH-EtOH and He mediums, respectively. Dashed lines show linear fits at each f_E range.

the first variation around 1 GPa is very clear with a change from a negative slope to a positive one, suggesting that a Lifshitz transition occurs in $PdTe_2$. Intriguingly, the negative slope at the lowest f_E range means that this range is stiffer than the higher-f_E ones: For example, $B_0 = 65.1(8)$ GPa at $f_E < 0.006$, 54(2) GPa at $0.006 < f_E < 0.008$, and 62.3(3) GPa at $0.008 < f_E$ in sample 1. Though this behavior is different from the general tendency under high pressure, we confirmed its reproducibility utilizing different mediums, and therefore we expect it to be intrinsic behavior.

Assuming that the topology of the Fermi surface changes around 1 GPa, we first consider the contribution of a saddle-point vHs, which sits ~30 meV above E_F near the M point [20], to the transition. This is because a vHs is regarded as a key feature for the emergence of superconductivity in $PdTe_2$ [14]. According to Kim *et al.*, the vHs band strongly correlates with the Te-shear $O_{1,2}$ phonon mode (in-plane vibrational mode), which tunes the intralayer Pd-Te spacing [14]. They theoretically estimated the energy shift (dE) versus Te displacement from the equilibrium position (dx) and the downshift of the vHs band to E_F by shrinkage of the intralayer Pd-Te spacing. Referring to their dx versus dE calculation as a rough guide, dx of ~0.1 Å is necessary to make the vHs band shift close to E_F. The estimated dx is significantly larger than the shrinkage amount in intralayer atomic spacings around 1 GPa. Indeed, they claimed that the modification of the Fermi surface near the M point will start at a 15% volume contraction [14], which corresponds to $P \sim 17$ GPa using B_0 of this study. Therefore, combined with the variation of the carrier density, it is unreasonable to interpret that the energy shift of the vHs band causes a Lifshitz transition around 1 GPa and thereby enhances T_c.

Fermi surface sheets of $PdTe_2$ are also positioned near the Γ and K points [14], and it is speculated that $H_v(f_E)$ is affected by them, particularly at the Γ point, where the phonon modes provide a large contribution to superconductivity [14]. Since the carrier density shows no remarkable changes around 1 GPa, we considered the factor of positive

dT_c/dP based on the pressure variation of Θ_D, which can also be linked to the change in $H_v(f_E)$. In general, for the same structure of the same substance, the pressure variation of the vibrational frequency tends to be smaller as the bulk modulus is higher. Therefore the pressure variation of Θ_D can be compatible with the variation of B_0 estimated from $H_v(f_E)$. From a structural point of view, perhaps the variation of the Te-Pd-Te angle, which shows a weak nonmonotonic behavior, leads to the change in compressibility. With regard to the superconducting properties, the pressure variations of the critical fields for the bulk and surface superconductivity, as well as those of T_c, have a maximum around 0.9–1.2 GPa (see the Supplementary Material in Ref. [24]). This suggests that the first variation of $H_v(f_E)$ around 1 GPa is reflected in the superconductivity. Meanwhile, the second variation of $H_v(f_E)$ around 1.5 GPa also has the possibility of a Lifshitz transition. In our previous ac-susceptibility measurement, the critical temperature of the surface superconductivity becomes higher than that of the bulk above 1.41 GPa [24]. This might be related to the electronic variation around 1.5 GPa in this paper. However, for a more reliable discussion, it is necessary to obtain detailed information on the electronic structure and phonon dispersions at lower pressures utilizing experimental structural parameters in future research.

V. SUMMARY AND CONCLUSION

We performed synchrotron radiation x-ray diffraction and electrical resistivity measurements on $PdTe_2$ under high pressure to investigate the effect of pressure on superconductivity up to 8 GPa and the origin of the nonmonotonic variation of T_c observed in our previous study [24]. With increasing pressure, T_c decreases from 1.8 K at 1 GPa to 0.82 K at 5.5 GPa with $dT_c/dP \sim -0.22$ K/GPa, and the pressure variation below 2.5 GPa is consistent with our previous results. Though a high-T_c phase beyond 4 K was observed above 3.7 GPa in one of the samples, we concluded that this transition is likely due to contamination with Te. As for the topological transition from a type-II Dirac semimetal to type I between 4.7 and 6.1 GPa theoretically predicted [23], no noticeable behavior relating to the transition is observed in the pressure variation of either $\rho(T)$ or superconductivity.

The pressure variation of T_c depends on the competition between the electronic density of states and lattice stiffening under pressure. In this paper, we found that Θ_D estimated from $\rho(T)$ exhibits insignificant changes up to pressures of $\sim$1 GPa and subsequently increases as a function of pressure. Considering this together with the moderate increase in carrier density at 2 K with pressure (see the Supplementary Material in Ref. [24]), we infer that the requirement for positive dT_c/dP is fulfilled below 1 GPa and, however, large stiffening depresses superconductivity above 1 GPa. On the other hand, the $P\bar{3}m1$ structure is maintained up to pressures of 8 GPa similar to reports in previous literature [22]. As a result of our strain analysis, we found a clear change in compressibility around 1 GPa, suggesting the possibility that the Fermi surface is modified by pressure. It can be considered that this affects the pressure variation of Θ_D, and eventually that of superconductivity. For a more solid discussion, further and more detailed information on the electronic structure of $PdTe_2$ at lower pressures is required.

ACKNOWLEDGMENTS

This work was partially supported by a Grant-in-Aid for Scientific Research, KAKENHI (No. 20H01851), and by the research program on Topological Insulators funded by (Dutch Foundation for Fundamental Research on Matter (FOM) and was performed under Proposal No. 2019G582 of Photon Factory, KEK. It was further supported by the Japan Society for the Promotion of Science (JSPS) Program for Fostering Globally Talented Researchers, Grant No. JPMXS05R2900003.

[1] A. A. Soluyanov, D. Gresch, Z. Wang, Q. Wu, M. Troyer, X. Dai, and B. A. Bernevig, Nature (London) **527**, 495 (2015).
[2] H. Huang, S. Zhou, and W. Duan, Phys. Rev. B **94**, 121117(R) (2016).
[3] M. S. Bahramy, O. J. Clark, B.-J. Yang, J. Feng, L. Bawden, J. M. Riley, I. Marković, F. Mazzola, V. Sunko, D. Biswas, S. P. Cooil, M. Jorge, J. W. Wells, M. Leandersson, T. Balasubramanian, J. Fujii, I. Vobornik, J. E. Rault, T. K. Kim, M. Hoesch *et al.*, Nat. Mater. **17**, 21 (2018).
[4] J. Guggenheim, F. Hulliger, and J. Müller, Helv. Phys. Acta **34**, 408 (1961).
[5] F. Fei, X. Bo, R. Wang, B. Wu, J. Jiang, D. Fu, M. Gao, H. Zheng, Y. Chen, X. Wang, H. Bu, F. Song, X. Wan, B. Wang, and G. Wang, Phys. Rev. B **96**, 041201(R) (2017).
[6] H.-J. Noh, J. Jeong, E.-J. Cho, K. Kim, B. I. Min, and B.-G. Park, Phys. Rev. Lett. **119**, 016401 (2017).
[7] O. J. Clark, M. J. Neat, K. Okawa, L. Bawden, I. Marković, F. Mazzola, J. Feng, V. Sunko, J. M. Riley, W. Meevasana, J. Fujii, I. Vobornik, T. K. Kim, M. Hoesch, T. Sasagawa, P. Wahl, M. S. Bahramy, and P. D. C. King, Phys. Rev. Lett. **120**, 156401 (2018).
[8] S. Das, Amit, A. Sirohi, L. Yadav, S. Gayen, Y. Singh, and G. Sheet, Phys. Rev. B **97**, 014523 (2018).
[9] Amit, R. K. Singh, N. Wadehra, S. Chakraverty, and Y. Singh, Phys. Rev. Materials **2**, 114202 (2018).
[10] H. Leng, C. Paulsen, Y. K. Huang, and A. de Visser, Phys. Rev. B **96**, 220506(R) (2017).
[11] Amit and Y. Singh, Phys. Rev. B **97**, 054515 (2018).
[12] M. V. Salis, P. Rodière, H. Leng, Y. K. Huang, and A. de Visser, J. Phys.: Condens. Matter **30**, 505602 (2018).
[13] S. Teknowijoyo, N. H. Jo, M. S. Scheurer, M. A. Tanatar, K. Cho, S. L. Bud'ko, P. P. Orth, P. C. Canfield, and R. Prozorov, Phys. Rev. B **98**, 024508 (2018).
[14] K. Kim, S. Kim, J. S. Kim, H. Kim, J.-H. Park, and B. I. Min, Phys. Rev. B **97**, 165102 (2018).
[15] T. Le, L. Yin, Z. Feng, Q. Huang, L. Che, J. Li, Y. Shi, and X. Lu, Phys. Rev. B **99**, 180504(R) (2019).
[16] J. A. Voerman, J. C. de Boer, T. Hashimoto, Y. K. Huang, C. Li, and A. Brinkman, Phys. Rev. B **99**, 014510 (2019).
[17] A. Sirohi, S. Das, P. Adhikary, R. R. Chowdhury, A. Vashist, Y. Singh, S. Gayen, T. Das, and G. Sheet, J. Phys.: Condens. Matter **31**, 085701 (2019).

[18] H. Leng, J.-C. Orain, A. Amato, Y. K. Huang, and A. de Visser, Phys. Rev. B **100**, 224501 (2019).
[19] M. V. Salis, Y. K. Huang, and A. de Visser, Phys. Rev. B **103**, 104502 (2021).
[20] E. van Heumen, M. Berben, L. Neubrand, and Y. K. Huang, Phys. Rev. Materials **3**, 114202 (2019).
[21] D. Saint-James and P. G. Gennes, Phys. Lett. **7**, 306 (1963).
[22] C. Soulard, P. E. Petit, P. Deniard, M. Evain, S. Jobic, M.-H. Whangbo, and A.-C. Dhaussy, J. Solid State Chem. **178**, 2008 (2005).
[23] R. C. Xiao, P. L. Gong, Q. S. Wu, W. J. Lu, M. J. Wei, J. Y. Li, H. Y. Lv, X. Luo, P. Tong, X. B. Zhu, and Y. P. Sun, Phys. Rev. B **96**, 075101 (2017).
[24] H. Leng, A. Ohmura, L. N. Anh, F. Ishikawa, T. Naka, Y. K. Huang, and A. de Visser, J. Phys.: Condens. Matter **32**, 025603 (2020).
[25] H. Yang, M. K. Hooda, C. S. Yadav, D. Hrabovsky, A. Gauzzi, and Y. Klein, Phys. Rev. B **103**, 235105 (2021).
[26] M. K. Hooda and C. S. Yadav, Europhys. Lett. **121**, 17001 (2018).
[27] K. Kudo, H. Ishii, and M. Nohara, Phys. Rev. B **93**, 140505(R) (2016).
[28] A. Lyons, D. Schleich, and A. Wold, Mater. Res. Bull. **11**, 1155 (1976).
[29] K. Takemura, P. Ch. Sahu, Y. Kunii, and Y. Toma, Rev. Sci. Instrum. **72**, 3873 (2001).
[30] H. M. Rietveld, Acta Crystallogr. **22**, 151 (1967).
[31] Crystallographic computing system JANA2006, http://jana.fzu.cz/.
[32] See Supplemental Material at http://link.aps.org/supplemental/10.1103/PhysRevB.104.144510 for detailed information on the Rietveld analysis of XRD patterns and the list of structural parameters, estimation of the Debye temperature, pressure variation of the electrical resistivity at room temperature, and estimation of the logarithmic volume derivative of the Hopfield parameter.
[33] T. Nakanishi, N. Takeshita, and N. Môri, Rev. Sci. Instrum. **73**, 1828 (2002).
[34] F. Ishikawa, K. Fukuda, S. Sekiya, A. Kaeriyama, Y. Yamada, and A. Matsushita, J. Phys. Soc. Jpn. **76**, 92 (2007).
[35] T. Nakanishi, M. Nicklas, G. Sparn, and F. Steglich, J. Phys. Soc. Jpn. **76**, 223 (2007).
[36] F. Birch, Phys. Rev. **71**, 809 (1947).
[37] B. Y. Shapiro, I. Shapiro, D. Li, and B. Rosenstein, J. Phys.: Condens. Matter **30**, 335403 (2018).
[38] I. V. Berman, Z. I. Bynzarov, and Y. P. Kurkin, Sov. Phys. Solid State **14**, 2192 (1973).
[39] H. Suderow, V. G. Tissen, J. P. Brison, J. L. Martinez, and S. Vieira, Phys. Rev. Lett. **95**, 117006 (2005).
[40] T. Li, K. Wang, C. Xu, Q. Hou, H. Wu, J.-Y. Ge, S. Cao, J. Zhang, W. Ren, X. Xu, N.-C. Yeh, B. Chen, and Z. Feng, arXiv:1911.07173.
[41] M. A. ElGhazali, P. G. Naumov, Q. Mu, V. Süß, A. O. Baskakov, C. Felser, and S. A. Medvedev, Phys. Rev. B **100**, 014507 (2019).
[42] M. A. ElGhazali, P. G. Naumov, H. Mirhosseini, V. Süß, L. Müchler, W. Schnelle, C. Felser, and S. A. Medvedev, Phys. Rev. B **96**, 060509(R) (2017).
[43] K. Gu, R. A. Susilo, F. Ke, W. Deng, Y. Wang, L. Zhang, H. Xiao, and B. Chen, J. Phys.: Condens. Matter **30**, 385701 (2018).
[44] B. Lorenz and C. W. Chu, in *Frontiers in Superconducting Materials*, edited by A. Narlikar (Springer-Verlag, Berlin, 2005), pp. 459–497.
[45] J. S. Schilling, in *Handbook of High-Temperature Superconductivity: Theory and Experiment*, edited by J. R. Schrieffer and J. S. Brooks (Springer, New York, 2007), pp. 427–462.
[46] I. M. Lifshitz, Sov. Phys. JETP **11**, 1130 (1960).
[47] B. K. Godwal, S. Speziale, S. M. Clark, J. Yan, and R. Jeanloz, J. Phys. Chem. Solids **71**, 1059 (2010).
[48] A. Polian, M. Gauthier, S. M. Souza, D. M. Trichês, J. Cardoso de Lima, and T. A. Grandi, Phys. Rev. B **83**, 113106 (2011).